

Supporting Information

Ferromagnetically coupled $\text{Co}^{\text{II}}_2\text{Ln}^{\text{III}}_2$ complexes (where $\text{Ln}^{\text{III}} = \text{Ho, Er, Yb}$): Experimental and theoretical investigations

Naushad Ahmed ^{a *} and Prem Prakash Sahu ^b

^a Department of Chemistry, Indian Institute of Technology Bombay, Powai, Mumbai, Maharashtra, India 400076. Email: naushad.chem@gmail.com

^b Department of Chemistry, Indian Institute of Technology Hyderabad, Kandi, Sangareddy, India 502285

Table S1. Crystallographic parameters for complexes **1** and **3**

Complex	1	3
Formula	$\text{C}_{74}\text{H}_{101}\text{N}_7\text{O}_{37}\text{Co}_2\text{Ho}_2$	$\text{C}_{74}\text{H}_{101}\text{N}_7\text{O}_{37}\text{Co}_2\text{Yb}_2$
Size [mm]	0.40 x 0.31 x 0.230	0.14 x 0.12 x 0.10
System	Monoclinic	Monoclinic
Space group	$C2/c$	$C2/c$
a [\mathring{A}]	26.692(7)	26.7585(7)
b [\mathring{A}]	15.981(4)	16.0409(5)
c [\mathring{A}]	19.803(5)	19.8206(6)
α [°]	90	90
β [°]	96.761(3)	96.400(3)
γ [°]	90	90
V [\mathring{A}³]	8389(4)	8454.6(4)
Z	4	4
ρ_{calcd} [g/cm³]	1.664	1.685
$2\theta_{\text{max}}$	49.98	50.00
radiation	Mo K _a	Mo K _a
λ [\mathring{A}]	0.71070	0.71070
T [K]	100	100
Reflns	11275	7455
Ind. Reflns	10035	6042
reflns with $I > 2\sigma(I)$	10035	11876
$R1$	0.0455	0.0413
$wR2$	0.0930	0.0946

Table S2. Continuous Shape Measurement (CShM) analysis for Ln1 and Co1 sites in complexes **1** and **3**

Geometry around Ln ^{III}	Ln1 site		Geometry around Ln ^{III}	Co1 site	
	Complex 1	Complex 2		Complex 1	Complex 2
OP-8	29.014	29.222	HP-6	33.681	33.549
HPY-8	23.361	23.140	PPY-6	21.898	21.910
HBPY-8	13.296	13.544	OC-6	2.133	2.203
CU-8	8.698	9.124	TPR-6	8.466	8.259
SAPR-8	1.553	1.586	JPPY-6	25.288	25.289
TDD-8	2.769	2.835			
JGBF-8	11.715	11.587			
JETBPY-8	25.321	24.873			
JBTPR-8	2.056	1.983			
BTPR-8	1.382	1.468			
JSD-8	4.102	3.624			
TT-8	9.455	9.840			
OP-8 D_{8h} Octagon, HPY-8 C_{7v} Heptagonal pyramid, HBPY-8 D_{6h} Hexagonal bipyramid, CU-8 O_h Cube, SAPR-8 D_{4d} Square antiprism, TDD-8 D_{2d} Triangular dodecahedron, JGBF-8 D_{2d} Johnson gyrobifastigium J26, JETBPY-8 D_{3h} Johnson elongated triangular bipyramid J14, JBTPR-8 C_{2v} Biaugmented trigonal prism J50, BTPR-8 C_{2v} Biaugmented trigonal prism, JSD-8 D_{2d} Snub diphenoïd J84, TT-8 Td Triakis tetrahedron, ETBPY-8 D_{3h} Elongated trigonal bipyramid	HP-6 D_{6h} Hexagon, PPY-6 C_{5v} Pentagonal pyramid, OC-6 O_h Octahedron, TPR-6 D_{3h} Trigonal prism, JPPY-6 C_{5v} Johnson pentagonal pyramid J2				

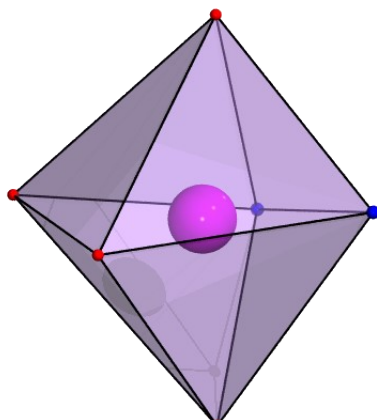
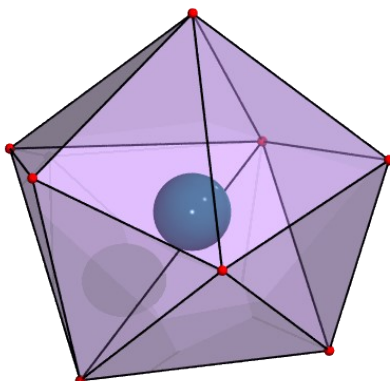


Table S3: Selected Bond angles and bond lengths for complexes **1** and **3**.

Bonds	1	3
Bond Lengths(Å)		
Co1-O11	2.043(4)	2.037(4)
Co1-N11	2.069(5)	2.056(5)
Co1-O13	2.144(4)	2.140(4)
Co1-N31	2.057(5)	2.051(5)
Co1-O31	2.065(4)	2.053(4)
Co1-O33	2.141(4)	2.138(4)
Ln1-O11	2.280(5)	2.241(4)
Ln1-O12	2.590(4)	2.576(4)
Ln1-O31	2.337(4)	2.312(4)
Ln1-O32	2.548(4)	2.535(4)
Ln1-O51	2.356(4)	2.227(4)
Ln1-O61	2.270(4)	2.317(4)
Ln1-O71	2.337(4)	2.286(4)
Ln1-O1w	2.340(5)	2.291(4)
Bond Angle (°)		
Co1-O11-Ln1	108.22(16)	108.10(15)
Co1-O31-Ln1	105.37(16)	104.93(15)
Dihedral Angle (°)		
Co1-O11-Ln1-O31	9.89	9.84
Intermetallic separation (Å)		
Co1-Ln1	3.505(4)	3.464(8)
Ln1-Ln1#	4.583(6)	4.579(5)

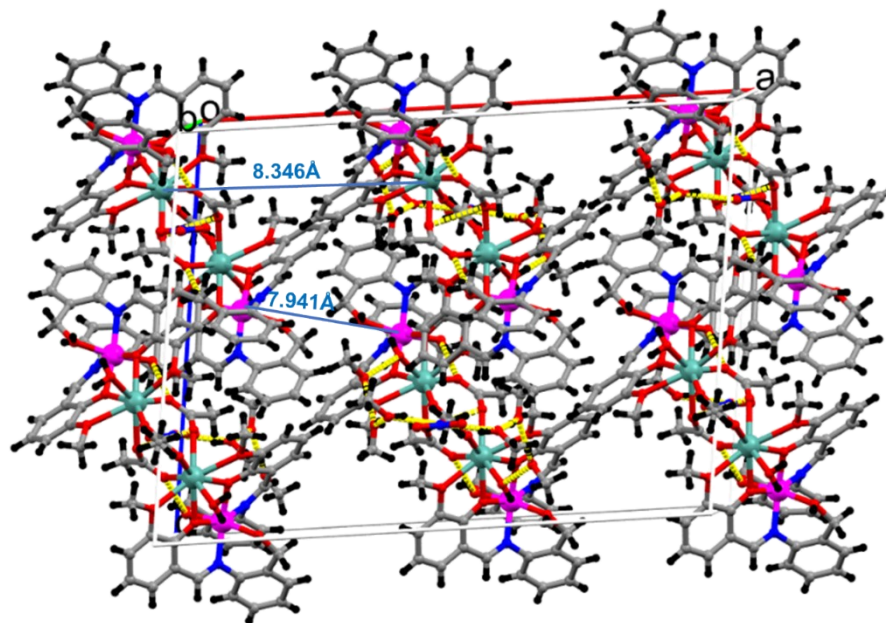


Figure S1. Packing structure of representative complex **1**. Yellow dotted bonds are the inter or intramolecular hydrogen bonding.

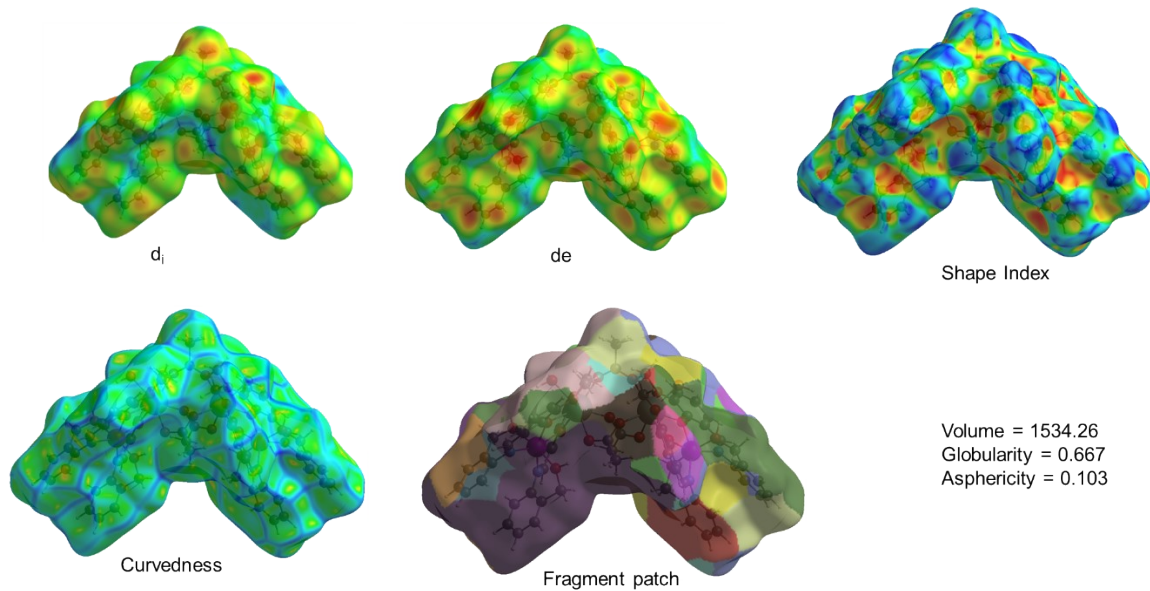


Figure S2. Different view of Hirshfeld surface analysis performed on complex **1**.

Computational Details

To rationalized our experimental findings, we have performed computational studies on all the complexes. The details of computational studies are below

Ab Initio calculations

All magnetic centers in **1**, **2^{mod}** and **3** were *ab initio* computed (irrespective of their crystallographic symmetry) using MOLCAS 8.0¹ software package. At a time one paramagnetic center kept active while rest of the centers replaced by diamagnetic counter parts i.e paramagnetic Ho^{III}, Er^{III} and Yb^{III} ions were replaced by diamagnetic Lu^{III} ions while paramagnetic Co^{II} ions by diamagnetic Zn^{II} ions. For calculations of the Spin-Hamiltonian parameters in the complete active space self-consistent field (CASSCF)² framework, the active space is comprised of the CAS (n,7) (where n = 10, 11, and 13, representing the number of active electrons in the seven 4f-based active orbitals of Ho^{III}, Er^{III}, and Yb^{III} for the Ln^{III} ion-centered respectively. CAS (7,5), i.e., seven active electrons in the five active d-orbitals, was employed for Co^{II}-ion 3d-center. The ANO-RCC library^{3, 4} was utilized for the basis set, with the complete basis set contraction scheme provided in Table S4. For Co^{II}, all the 10 quartet and 40 doubles states were taken into account during the computation procedure. For Ho^{III}, 35 quintets and 105 triplets were considered. Similarly, for Er^{III} 35 quartets and 112 doublets were taken while for Yb^{III} 7 doublets were used for CASSCF-framework computation. The computed spin-free states for each Ln^{III} center were subsequently mixed using a spin-orbit restricted active space spin-interaction (SO-RASSI)⁵ to calculate the spin-orbit states. These computed spin-orbit states were taken to the SINGLE_ANISO⁶ module to extract the g-values, crystal field parameters, ab initio blockade barrier, and d.c. magnetic properties (magnetic susceptibility and magnetization). Resolution of identity Cholesky decomposition (RICD)⁷ was turned on to save the disk space. Lastly using the POLY_ANISO^{8, 9} module, dc magnetic properties were simulated to extract the magnetic exchange interaction (dipolar + exchange contribution) between the Co-Ln and Ln-Ln pairs respectively.

BS-DFT calculations

We used an all-electron scalar relativistic effect (SARC) basis set for Gd¹⁰ and Douglas-Kroll-Hess approximation,¹¹ DKH-adapted reconstructed versions of def2-type basis sets for the remaining atoms; DKH-def2-TZVPP for Co^{II}; DKH-def2-TZVP for the atoms in the first coordination sphere (N and O), and DKH-def2-SVP for C, and H atoms. Grimme's dispersion with Becke-Johnson damping (D3BJ)^{12, 13} was incorporated to account for the dispersion interaction as implemented in the ORCA. The resolution-of-identity-chain-of-spheres (RIJCOSX) formalism, along with the large GRID setting "GRID6" criterion, was turned on to speed up the calculations.^{14, 15} The spin-flip method included within ORCA was used to carry out BS-DFT by flipping the spin of the Co^{II} center.

Table S4. Basis set used in calculations using MOLCAS 8.0 code.

Element	Basis set
C	ANO-RCC...3s2p.
H	ANO-RCC...2s.
N , O	ANO-RCC...3s2p1d.
Zn	ANO-RCC...5s4p2d.
Co	ANO-RCC...6s5p3d2f1g.
Ho, Er, Yb	ANO-RCC...8s7p5d3f2g1h.
Lu	ANO-RCC...7s6p4d2f.

Table S5. The CASSCF computed g-tensors along with the axial (D) and transverse (E) magnetic

	g_x	g_y	g_z	D / cm ⁻¹	E / cm ⁻¹	E/D
Complex 1						
Co1	2.0545	2.3385	2.8056	-58.8310	17.9966	0.3059
Co2	2.0523	2.3407	2.8048	-58.8216	17.9970	0.3059
Complex 3						
Co1	2.0219	2.3055	2.8704	-67.5027	17.7658	0.2630
Co2	2.0283	2.3014	2.8676	-67.4912	17.7604	0.2631

anisotropies for Co(II) ions in complexes **1** and **3**.

Table S6. SO-RASSI computed low lying energies (cm⁻¹) of spin-free states of the individual Co^{II} centers in complexes **1** and **3**.

Complex 1		Complex 3	
Co1		Co1	
0	30636.524	0	30808.262
799.196	31193.686	693.07	31303.437
1708.773	32294.969	1815.925	32519.02
6404.823	32905.526	6773.563	33025.821
7983.502	34440.085	8216.427	34699.434
8420.809	35264.171	8573.837	35657.419
15518.956	35480.63	15950.87	35757.872
23007.096	35636.942	23241.001	35862.744
24689.428	36734.475	24876.335	37099.152
26271.890	36794.611	26416.522	37165.289
13614.934	36993.019	13399.338	37390.845
16315.56	37146.651	15943.791	37571.14
19379.376	46652.758	19438.198	46741.601

19713.053	47465.896	19715.907	47457.405
20365.051	47705.492	20366.832	47839.085
20853.583	48409.004	20822.984	48485.136
21316.839	48908.18	21259.323	49085.359
21818.008	49334.074	21758.109	49524.109
25430.008	49607.916	25475.504	49829.802
25517.322	71219.552	25741.406	71427.106
26147.629	71659.525	26154.675	71758.857
26530.777	72366.991	26587.024	72469.482
28667.922	74369.79	28756.959	74490.336
29383.423	74610.191	29453.819	74749.969
29694.007		29868.227	
30424.319		30673.723	

Table S7. SO-RASSI computed low lying energies (cm^{-1}) of spin-orbit states of Co1 center in complex **1**.

Complex 1				
Co1 site				
0	15814.081	25690.699	35437.422	49919.469
133.141	15814.081	26273.191	35437.422	71503.596
133.141	16547.039	26273.191	35679.607	71503.596
936.801	16547.039	26641.457	35679.607	71941.284
936.801	19585.586	26641.457	36166.374	71941.284
1165.192	19585.586	26852.544	36166.374	72701.36
1165.192	19984.423	26852.544	36863.358	72701.36
1948.59	19984.423	27240.011	36863.358	74577.013
1948.59	20578.675	27240.011	37154.472	74577.013
2051.68	20578.675	28940.863	37154.472	75023.619
2051.68	21173.838	28940.863	37432.181	75023.619
6643.254	21173.838	29717.303	37432.181	
6643.254	21603.887	29717.303	37798.643	

6717.653	21603.887	29991.72	37798.643	
6717.653	22189.448	29991.72	46869.897	
8195.253	22189.448	30673.591	46869.897	
8195.253	23117.136	30673.591	47708.293	
8249.839	23117.136	30993.01	47708.293	
8249.839	23194.013	30993.01	48048.529	
8651.834	23194.013	31442.328	48048.529	
8651.834	24697.081	31442.328	48690.29	
8758.885	24697.081	32639.811	48690.29	
8758.885	24864.525	32639.811	49145.877	
13857.001	24864.525	33202.643	49145.877	
13857.001	25467.831	33202.643	49662.195	
15808.699	25467.831	34642.092	49662.195	
15808.699	25690.699	34642.092	49919.469	

Table S8. SO-RASSI computed low lying energies (cm^{-1}) of spin-orbit states of Co1 center in complex **3**.

Complex 3				
Co1 site				
0	16188.603	25895.436	34925.708	50155.745
0	16254.009	25895.436	35770.318	50155.745
148.371	16254.009	26402.28	35770.318	71720.643
148.371	16265.05	26402.28	35971.946	71720.643
869.256	16265.05	26755.517	35971.946	72064.453
869.256	19651.836	26755.517	36496.579	72064.453
1108.661	19651.836	26909.067	36496.579	72818.523
1108.661	20005.954	26909.067	37249.144	72818.523
2058.546	20005.954	27386.182	37249.144	74715.88
2058.546	20596.586	27386.182	37577.764	74715.88
2158.859	20596.586	29058.639	37577.764	75176.758
2158.859	21165.679	29058.639	37816.096	75176.758

7024.504	21165.679	29827.695	37816.096	
7024.504	21565.788	29827.695	38194.736	
7096.518	21565.788	30156.035	38194.736	
7096.518	22146.724	30156.035	46968.503	
8442.583	22146.724	30940.933	46968.503	
8442.583	23354.579	30940.933	47740.346	
8494.768	23354.579	31174.046	47740.346	
8494.768	23439.748	31174.046	48181.398	
8822.642	23439.748	31574.004	48181.398	
8822.642	24878.296	31574.004	48782.93	
8931.83	24878.296	32867.395	48782.93	
8931.83	25061.402	32867.395	49343.248	
13660.448	25061.402	33342.73	49343.248	
13660.448	25581.699	33342.73	49865.479	
16188.603	25581.699	34925.708	49865.479	

Table S9. SO-RASSI computed low lying energies (cm^{-1}) of spin-free states of Ho1 center in complex 1.

Ho1 site				
0	45633.692	27475.796	32445.109	37385.957
10.015	45735.348	29477.792	32478.752	38944.94
100.898	45881.127	29498.982	33366.807	38946.647
134.381	46186.391	29524.818	33408.249	38948.139
148.065	46251.729	29538.145	33475.996	38950.213
180.54	21435.006	29570.977	35565.372	38961.159
231.855	21435.422	29578.851	35565.381	38963.242
277.943	21445.893	29598.374	35743.156	38969.965
307.655	21446.922	29652.892	35743.259	38982.482
310.646	21450.96	29655.398	35834.665	38985.349
339.432	21451.192	29819.839	35835.978	38996.996
393.583	21458.59	29819.941	35903.349	38998.497

406.579	21459.021	29892.267	35908.818	39001.46
17790.063	21464.836	29893.156	35965.195	39001.641
17848.251	21472.932	29979.933	35973.234	44728.023
17977.741	21477.931	29984.572	36011.314	44757.343
17992.86	21484.125	30005.549	36014.77	44892.357
18001.952	21485.935	30026.716	36023.002	44957.193
18042.585	21491.857	30035.01	36073.891	44999.397
18125.068	21492.272	30063.903	36079.827	45156.251
18156.454	27204.143	30071.339	36204.08	45186.666
27983.761	27207.785	30104.238	36205.138	
28034.449	27275.28	30105.215	36315.908	
28049.967	27287.129	30119.136	36316.068	
28083.102	27323.751	30119.158	37012.637	
28149.768	27335.669	30210.751	37101.443	
28175.113	27372.798	30210.78	37175.172	
28251.01	27390.77	32287.579	37213.195	
28350.01	27396.726	32301.456	37311.69	
28360.173	27475.071	32399.005	37375.091	

Table S10. SO-RASSI computed low lying energies (cm^{-1}) of spin-orbit states of Ho1 center in complex 1

Ho1 site																
0	5336.748	13943.957	25505.958	27468.783	30301.608	33051.38	33795.137	38079.663	39106.727	41757.919	42841.727	45123.975	46167.283	47741.938	48727.619	54363.627
0.935	5336.755	13960.885	25506.367	27537.724	30303.323	33058.484	33797.949	38082.39	39122.835	41769.499	42842.667	45182.103	46167.828	47743.049	48736.046	54387.451
65.889	8871.104	14000.888	25513.937	28903.606	30331.571	33059.396	33806.877	38095.05	39333.847	41775.707	42903.629	45189.124	46710.343	47875.672	48742.936	55753.123
68.568	8871.342	14049.905	25515.158	28903.69	30342.17	33092.58	33813.174	38116.591	39356.62	41781.22	42904.792	45224.808	46720.893	47893.596	48747.493	55760.784
108.956	8912.048	14063.74	25520.028	28907.054	30348.759	33092.622	33820.143	38126.813	39368.274	41785.585	42973.927	45242.288	46738.964	47953.002	48754.599	55796.472
112.429	8914.118	20579.804	25520.875	28908.299	30367.818	33157.373	34529.112	38146.034	39375.536	41794.412	42998.527	45254.787	46908.204	47976.429	48762.378	55850.313
153.158	8925.238	20580.123	25522.065	28909.908	30378.869	33157.509	34533.776	38150.098	39386.212	41806.961	43012.1	45305.11	46917.245	47990.971	48764.923	55863.909
178.478	8930.759	20638.325	25522.766	28911.859	30404.624	33222.362	34548.569	38517.225	39403.639	41903.54	43043.054	45306.425	46925.616	48053.677	48772.175	56575.309
191.694	8948.665	20641.953	25524.917	28913.469	30407.986	33222.826	34554.211	38517.239	39417.49	41904.33	43055.03	45391.223	46938.025	48061.176	48778.589	56710.32
197.216	8959.154	20683.799	25525.485	28914.617	30436.904	33250.24	34562.207	38581.457	40166.797	41957.986	43079.865	45391.331	46951.651	48151.603	48780.234	56886.279
214.523	8966.026	20699.321	25531.824	28915.595	30437.49	33254.583	34566.273	38581.771	40166.799	41965.183	43085.927	45488.352	46967.338	48151.845	48787.797	57165.18
221.431	9001.869	20715.068	25534.221	28917.226	32843.831	33277.309	34579.124	38651.287	40326.975	41995.797	43089.788	45488.359	46969.986	48277.128	48794.088	57386.04
225.312	9003.42	20738.231	25535.164	28918.408	32847.802	33288.795	34595.29	38655.927	40327.002	42015.382	43095.15	45529.433	46974.502	48277.345	48803.768	57394.038
244.91	9046.342	20741.022	25538.909	28920.119	32867.944	33303.341	34595.624	38674.751	40418.832	42029.131	43179.312	45540.634	46980.466	48388.667	48810.263	57493.454
247.171	9046.657	20779.485	25540.077	28921.87	32884.44	33321.562	34598.932	38678.784	40419.201	42060.545	43179.84	45581.597	47206.508	48389.135	48877.794	57518.524
316.575	11641.059	20779.62	25551.357	28926.102	32889.498	33325.263	34602.897	38693.503	40480.399	42068.358	43705.627	45624.044	47208.255	48465.599	48878.083	57556.443
316.78	11641.581	23616.625	25551.431	28927.299	32893.003	33363.912	36590.141	38696.073	40482.443	42135.217	43714.346	45631.747	47232.79	48466.609	53591.59	57635.322
5139.382	11680.406	23617.207	25723.038	29496.26	32902.883	33364.565	36631.617	38703.389	40542.148	42135.583	43788.09	46094.469	47239.163	48509.269	53592.939	57646.227
5139.524	11683.097	23621.376	25732.577	29497.459	32932.645	33408.042	36660.335	38713.927	40546.733	42479.875	43789.423	46094.604	47253.334	48522.565	53663.455	63036.041
5179.429	11700.571	23625.988	25757.02	29519.67	32941.311	33408.183	36667.273	38726.311	40589.301	42841.727	43822.754	46113.913	47720.08	48535.611	53677.894	63061.666
5180.588	11709.33	23626.33	25783.968	29524.503	33001.288	33482.008	36675.734	38733.531	40598.102	42842.667	43850.478	46114.551	47720.656	48578.77	53709.869	63185.643
5212.894	11723.446	23814.87	25796.918	29532.563	33002.655	33482.019	36700.937	38734.947	40615.359	42903.629	43869.049	46121.241	47722.669	48580.975	53790.442	63326.605
5221.034	11756.125	23815.821	25836.91	29536.963	33007.462	33714.512	36720.476	38743.861	40628.82	42904.792	43949.236	46123.214	47726.132	48656.984	53801.67	63337.902
5226.816	11759.363	23851.549	25849.675	29546.634	33011.629	33718.27	37081.479	38772.629	40630.951	42973.927	43950.91	46129.561	47727.423	48657.743	53956.839	
5236.798	11807.008	23869.553	26775.613	29559.673	33017.439	33736.183	37091.505	38773.997	40697.546	42998.527	44808.02	46135.642	47728.177	48667.221	53959.977	
5245.621	11808.51	23905.049	26788.936	29572.485	33020.282	33744.443	37140.742	38799.467	40699.605	43012.1	44808.024	46142.7	47730.326	48667.721	54193.546	
5261.723	13815.272	23926.756	26812.333	29587.829	33025.812	33752.747	37210.148	38799.652	40815.049	43043.054	44947.91	46148.85	47732.568	48696.424	54206.46	

5263.752	13843.327	23933.668	26849.428	29591.671	33039.343	33760.776	37212.408	38879.564	40815.354	43055.03	44947.96	46152.279	47733.564	48698.348	54263.459	
5285.421	13914.743	23965.441	26855.857	29625.838	33041.152	33769.444	38056.488	38879.597	40910.858	43079.865	45046.461	46156.103	47736.349	48709.726	54274.426	
5285.674	13925.715	23970.706	27410.233	29626.241	33051.01	33785.902	38062.403	39089.325	40910.912	43085.927	45047	46156.812	47740.212	48713.714	54323.461	

Table S11. SO-RASSI computed low lying energies (cm⁻¹) of spin-free and spin-orbit states of Yb1 center in complex **3**.

Yb1 site		
Spin-free	Spin-orbit state	
0.00	0.00	439.702
82.922	0.00	10336.058
288.233	199.746	10336.058
314.503	199.746	10539.773
378.773	321.035	10539.773
503.839	321.035	10699.771
532.738	439.702	10699.771

Table S12. SINGLE_ANISO computed wave function decomposition analysis for Ho1 center in complex

1. The major dominating values are kept in bold.

$\pm mJ$	<i>wave function decomposition analysis Ho1</i>
1	56.0% $ \pm 8\rangle$ + 23.6% $ \pm 6\rangle$ + 15.9% $ \pm 7\rangle$
2	53.0% $ \pm 7\rangle$ + 23.0% $ \pm 5\rangle$ + 9.4% $ \pm 6\rangle$ + 4.9% $ \pm 8\rangle$ + 4.0% $ \pm 3\rangle$
3	45.3% $ \pm 2\rangle$ + 21.0% $ 0\rangle$ + 14.5% $ \pm 3\rangle$ + 10.8% $ \pm 4\rangle$
4	46.1% $ 0\rangle$ + 15.1% $ \pm 2\rangle$ + 12.4% $ \pm 6\rangle$ + 10.0% $ \pm 3\rangle$ + 9.2% $ \pm 8\rangle$
5	29.5% $ \pm 4\rangle$ + 17.1% $ \pm 6\rangle$ + 16.9% $ \pm 8\rangle$ + 10.0% $ \pm 1\rangle$ + 8.5% $ \pm 5\rangle$ + 7.6% $ \pm 7\rangle$ + 5.7% $ \pm 2\rangle$ + 4.1% $ \pm 3\rangle$
6	27.8% $ \pm 3\rangle$ + 24.3% $ \pm 4\rangle$ + 13.3% $ \pm 7\rangle$ + 13.0% $ \pm 1\rangle$ + 8.0% $ \pm 5\rangle$ + 4.8% $ 0\rangle$
7	29.3% $ \pm 5\rangle$ + 17.0% $ \pm 4\rangle$ + 13.4% $ \pm 6\rangle$ + 13.4% $ \pm 3\rangle$ + 9.8% $ \pm 8\rangle$ + 6.7% $ \pm 7\rangle$ + 4.5% $ \pm 1\rangle$
8	35.3% $ \pm 6\rangle$ + 26.7% $ \pm 2\rangle$ + 22.8% $ \pm 3\rangle$ + 10.5% $ \pm 4\rangle$
9	35.7% $ \pm 1\rangle$ + 27.3% $ \pm 3\rangle$ + 16.0% $ 0\rangle$ + 12.8% $ \pm 1\rangle$ + 5.6% $ \pm 4\rangle$

Table S13. SINGLE_ANISO computed wave function decomposition analysis for Er1 center in complex **2^{mod}**. The major dominating values are kept in bold.

$\pm mJ$	wave function decomposition analysis on Er1
KD1	84.7% $ \pm 15/2\rangle$ + 8.4% $ \pm 9/2\rangle$
KD2	29.4% $ \pm 7/2\rangle$ + 27.1% $ \pm 5/2\rangle$ + 12.3% $ \pm 1/2\rangle$ + 9.4% $ \pm 3/2\rangle$ + 6.8% $ \pm 11/2\rangle$ + 5.9% $ \pm 13/2\rangle$ + 5.3% $ \pm 9/2\rangle$
KD3	44.8% $ \pm 13/2\rangle$ + 18.1% $ \pm 11/2\rangle$ + 7.6% $ \pm 9/2\rangle$ + 7.1% $ \pm 7/2\rangle$ + 7.0% $ \pm 5/2\rangle$ + 7.0% $ \pm 3/2\rangle$ + 6.0% $ \pm 1/2\rangle$
KD4	23.2% $ \pm 3/2\rangle$ + 20.6% $ \pm 9/2\rangle$ + 19.2% $ \pm 11/2\rangle$ + 16.0% $ \pm 1/2\rangle$ + 9.7% $ \pm 7/2\rangle$ + 6.4% $ \pm 13/2\rangle$
KD5	25.8% $ \pm 9/2\rangle$ + 20.1% $ \pm 13/2\rangle$ + 18.3% $ \pm 11/2\rangle$ + 16.5% $ \pm 5/2\rangle$ + 12.0% $ \pm 3/2\rangle$ + 4.4% $ \pm 15/2\rangle$
KD6	22.8% $ \pm 11/2\rangle$ + 20.6% $ \pm 9/2\rangle$ + 19.0% $ \pm 13/2\rangle$ + 18.4% $ \pm 7/2\rangle$ + 7.2% $ \pm 1/2\rangle$ + 6.0% $ \pm 5/2\rangle$ + 5.6% $ \pm 3/2\rangle$
KD7	31.7% $ \pm 5/2\rangle$ + 26.1% $ \pm 7/2\rangle$ + 18.4% $ \pm 1/2\rangle$ + 8.8% $ \pm 11/2\rangle$ + 6.8% $ \pm 9/2\rangle$ + 5.6% $ \pm 3/2\rangle$
KD8	37.3% $ \pm 1/2\rangle$ + 36.5% $ \pm 3/2\rangle$ + 15.1% $ \pm 5/2\rangle$ + 4.8% $ \pm 9/2\rangle$

Table S14. SINGLE_ANISO computed wave function decomposition analysis for Yb1 center in complex **3**. The major dominating values are kept in bold.

$\pm mJ$	wave function decomposition analysis Yb1
KD1	83.2% $ \pm 7/2\rangle$ + 11.0% $ \pm 3/2\rangle$
KD2	77.0% $ \pm 5/2\rangle$ + 10.8% $ \pm 1/2\rangle$ + 10.4% $ \pm 3/2\rangle$
KD3	51.8% $ \pm 3/2\rangle$ + 23.9% $ \pm 1/2\rangle$ + 12.5% $ \pm 7/2\rangle$ + 11.7% $ \pm 5/2\rangle$
KD4	63.2% $ \pm 1/2\rangle$ + 26.2% $ \pm 3/2\rangle$ + 8.0% $ \pm 5/2\rangle$

Table S15. BS-DFT computed energies of high-spin and broken-symmetry solution of Co-Gd analogue centers for complex **1** using $H = -2J(S_1S_2)$ formalism.

Solution	Energy (E_h)	ρ^{Gd1}	ρ^{Co2}	$\langle S^{**2} \rangle$	J_{Co-Gd} (cm^{-1})	J_{Co-Ho} [(4/7)* J_{Co-Gd}] (cm^{-1})
HS	-15139.169025921756	7.016	2.678	30.0154	0.40	0.23
BS	-15139.168987786079	7.016	-2.678	9.0153		

J values are estimated using the following equation,

$$J = -\frac{E_{HS} - E_{BS}}{\langle S^{**2} \rangle_{HS} - \langle S^{**2} \rangle_{BS}}$$

Table S16. BS-DFT computed energies of high-spin and broken-symmetry solution of Co-Gd analogue centres for Co-Yb in complex **3** using $H = -2J(S_1S_2)$ formalism.

Solution	Energy (E_h)	ρ^{Gd1}	ρ^{Co2}	$\langle S^{**2} \rangle$	J_{Co-Gd} (cm^{-1})	J_{Co-Yb} [(1/7)* J_{Co-Gd}] (cm^{-1})
HS	-15139.128358439193	7.011	2.671	30.0155	0.38	0.05
BS	-15139.128322032311	7.010	-2.670	9.0153		

Table S17. DFT computed overlap integral values for the seven corresponding 3d-4f orbitals between Co-Gd analogue centers for complex **1**.

Corresponding 3d-4f orbitals	Overlap Integral value (S_{ab})
227	0.01812
228	0.01434
229	0.00890
230	0.00000
231	0.00000
232	-0.00000
233	-0.00000

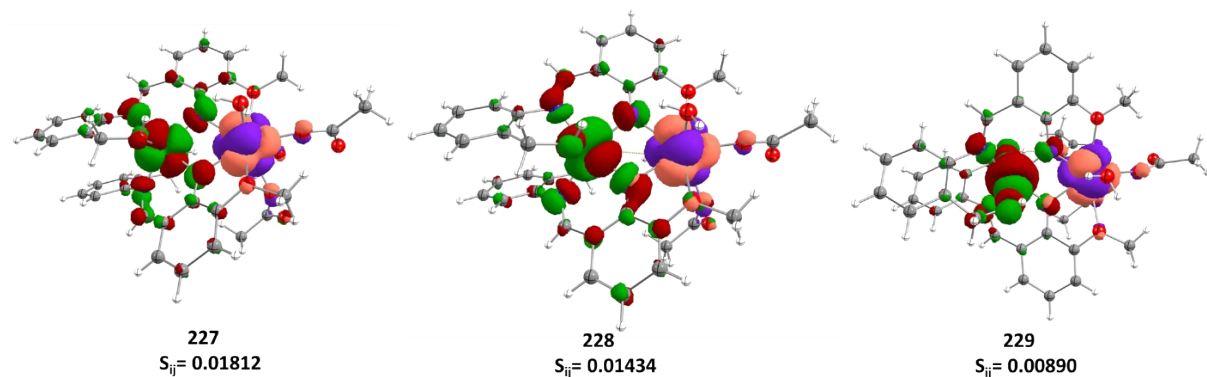


Figure S4. The three unrestricted corresponding orbitals (UCO) representing the strongest overlap between the 3d-4f orbitals of Co-Gd analogue centers for complex **1**. The iso-surface value = 0.03 e⁻/bohr³.

Table S18. DFT computed overlap integral values for the seven corresponding 3d-4f orbitals between Co-Gd analogue centers for complex **3**.

Corresponding 3d-4f orbitals	Overlap Integral value (S_{ab})
227	0.01936
228	0.01529
229	0.00974
230	-0.00000
231	-0.00000
232	0.00000
233	0.00000

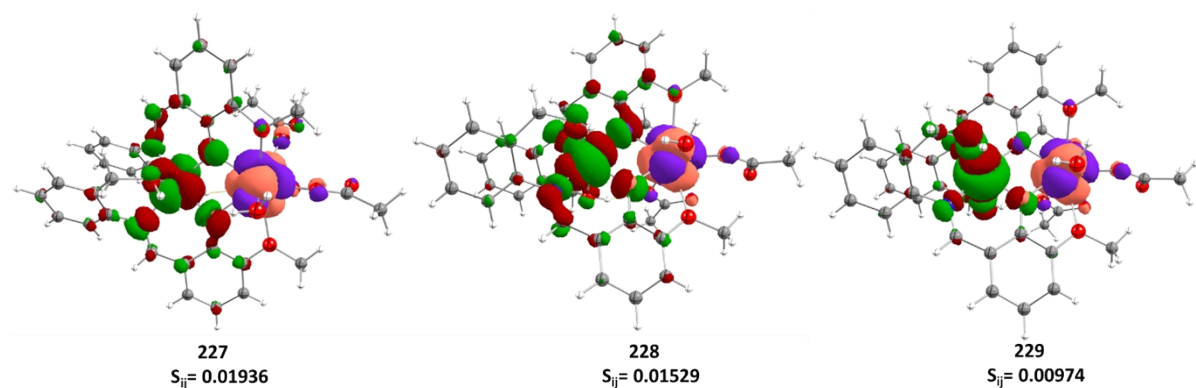


Figure S5. The three unrestricted corresponding orbitals (UCO) representing the strongest overlap between the 3d-4f orbitals of Co-Gd analogue centers for complex **3**. The iso-surface value = 0.03 e⁻/bohr³.

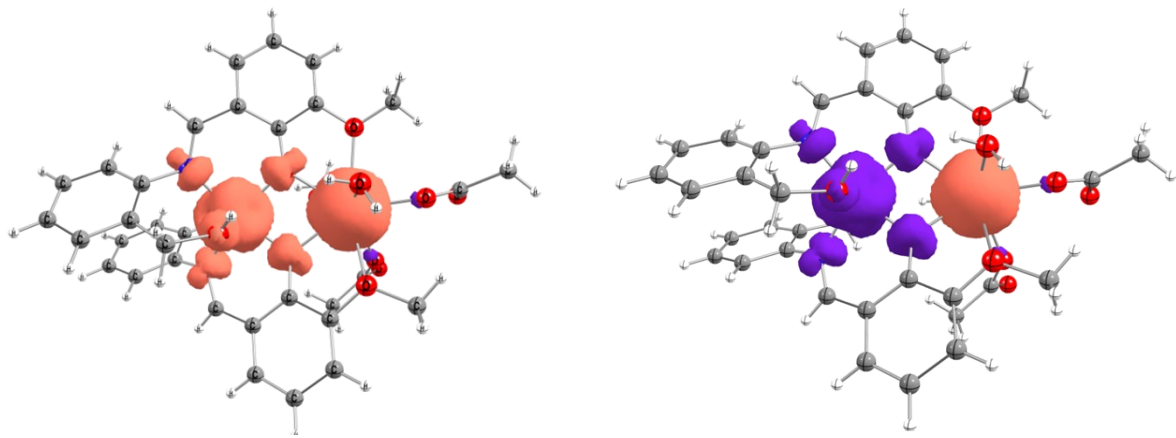


Figure S6. DFT computed spin-density plot for Co-Gd analogue centers for complex **1**. The iso-density surface here is constructed with a contour value of $0.002 \text{ e}^-/\text{bohr}^3$. The orange and purple colour represents the positive and negative spin densities respectively.

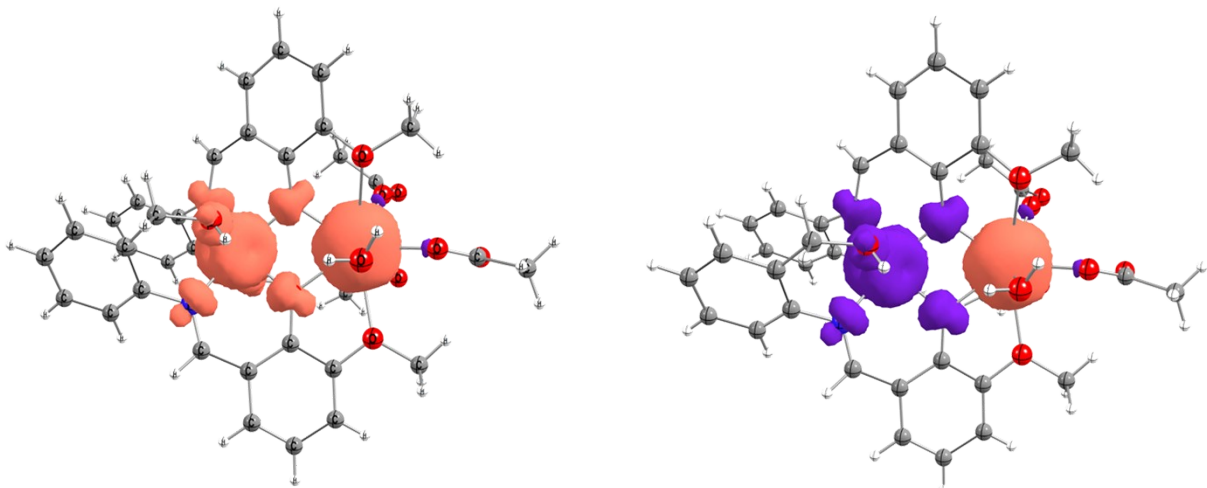


Figure S7. DFT computed spin-density plot for Co-Gd analogue centers for complex **3**. The iso-density surface here is constructed with a contour value of $0.002 \text{ e}^-/\text{bohr}^3$. The orange and purple colour represents the positive and negative spin densities respectively.

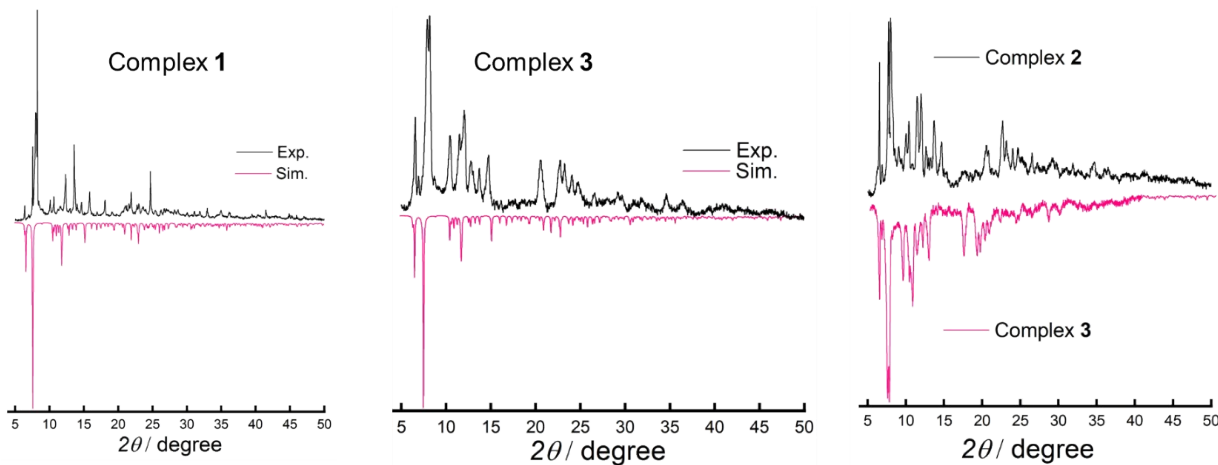


Figure S8. Powder X-ray diffraction analysis of complexes **1-3**.

References

1. F. Aquilante, J. Autschbach, R. K. Carlson, L. F. Chibotaru, M. G. Delcey, L. De Vico, I. Fdez. Galván, N. Ferré, L. M. Frutos and L. Gagliardi, Molcas 8: New capabilities for multiconfigurational quantum chemical calculations across the periodic table. *Journal*, 2016.
2. B. O. Roos, P. R. Taylor and P. E. Sigbahn, A complete active space SCF method (CASSCF) using a density matrix formulated super-CI approach, *Chem. Phys.*, 1980, **48**, 157-173.
3. B. O. Roos, V. Veryazov and P.-O. Widmark, Relativistic atomic natural orbital type basis sets for the alkaline and alkaline-earth atoms applied to the ground-state potentials for the corresponding dimers, *Theo. Chem. Acc.*, 2004, **111**, 345-351.
4. B. r. O. Roos, R. Lindh, P.-Å. Malmqvist, V. Veryazov, P.-O. Widmark and A. C. Borin, New relativistic atomic natural orbital basis sets for lanthanide atoms with applications to the Ce diatom and LuF₃, *J. Phys. Chem. A*, 2008, **112**, 11431-11435.
5. P. Å. Malmqvist, B. O. Roos and B. Schimmelpfennig, The restricted active space (RAS) state interaction approach with spin-orbit coupling, *Chem. Phys. Lett.*, 2002, **357**, 230-240.
6. L. F. Chibotaru and L. Ungur, *Ab initio* calculation of anisotropic magnetic properties of complexes. I. Unique definition of pseudospin Hamiltonians and their derivation, *J. Chem. Phys.*, 2012, **137**.
7. F. Aquilante, R. Lindh and T. Bondo Pedersen, Unbiased auxiliary basis sets for accurate two-electron integral approximations, *J. Chem. Phys.*, 2007, **127**, 114107.

8. L. F. Chibotaru, L. Ungur, C. Aronica, H. Elmoll, G. Pilet and D. Luneau, Structure, magnetism, and theoretical study of a mixed-valence $\text{Co}^{\text{II}}_3\text{Co}^{\text{III}}_4$ heptanuclear wheel: Lack of SMM behavior despite negative magnetic anisotropy, *J. Am. Chem. Soc.*, 2008, **130**, 12445-12455.
9. L. F. Chibotaru, L. Ungur and A. Soncini, The origin of nonmagnetic Kramers doublets in the ground state of dysprosium triangles: evidence for a toroidal magnetic moment, *Angew. Chem.*, 2008, **120**, 4194-4197.
10. D. A. Pantazis and F. Neese, All-Electron Scalar Relativistic Basis Sets for the Lanthanides, *Journal of Chem. Theo. Comput.*, 2009, **5**, 2229-2238.
11. B. A. Hess, Relativistic electronic-structure calculations employing a two-component no-pair formalism with external-field projection operators, *Phys. Rev. A*, 1986, **33**, 3742.
12. S. Grimme, J. Antony, S. Ehrlich and H. Krieg, A consistent and accurate ab initio parametrization of density functional dispersion correction (DFT-D) for the 94 elements H-Pu, *J. Chem. Phys.*, 2010, **132**.
13. S. Grimme, S. Ehrlich and L. Goerigk, Effect of the damping function in dispersion corrected density functional theory, *J. Comput. Chem.*, 2011, **32**, 1456-1465.
14. R. Izsák and F. Neese, An overlap fitted chain of spheres exchange method, *J. Chem. Phys.*, 2011, **135**.
15. R. Izsák and F. Neese, Speeding up spin-component-scaled third-order perturbation theory with the chain of spheres approximation: the COSX-SCS-MP3 method, *Mol. Phys.*, 2013, **111**, 1190-1195.